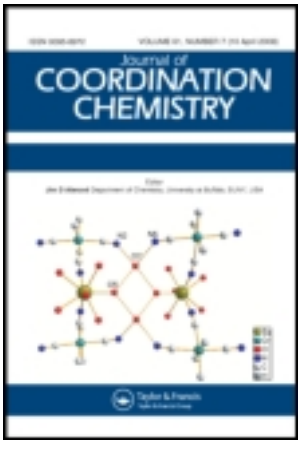

Journal of Coordination Chemistry
Publication details, including instructions for authors and subscription information:
http://www.tandfonline.com/loi/gcoo20

Spectroscopic, catalytic, and biological studies on mononuclear ruthenium(II) ONSN chelating thiosemicarbazone complexes

G. Raja [a], N. Sathya [a] & C. Jayabalakrishnan [a]
[a] Post Graduate and Research Department of Chemistry, Sri Ramakrishna Mission Vidyalaya College of Arts and Science, Coimbatore - 641 020, Tamil Nadu, India
Version of record first published: 18 Feb 2011.

To cite this article: G. Raja, N. Sathya & C. Jayabalakrishnan (2011): Spectroscopic, catalytic, and biological studies on mononuclear ruthenium(II) ONSN chelating thiosemicarbazone complexes, Journal of Coordination Chemistry, 64:5, 817-831

To link to this article: http://dx.doi.org/10.1080/00958972.2011.556721

Journal of Coordination Chemistry
Vol. 64, No. 5, 10 March 2011, 817–831

Taylor & Francis
Taylor & Francis Group

Spectroscopic, catalytic, and biological studies on mononuclear ruthenium(II) ONSN chelating thiosemicarbazone complexes

G. RAJA, N. SATHYA and C. JAYABALAKRISHNAN*

Post Graduate and Research Department of Chemistry, Sri Ramakrishna Mission Vidyalaya College of Arts and Science, Coimbatore – 641 020, Tamil Nadu, India

(*Received 18 June 2010; in final form 3 December 2010*)

A group of new ruthenium(II) thiosemicarbazone complexes, [Ru(CO)(B)(L)] (where B = PPh_3/$AsPh_3$/Py; L = dibasic tetradentate Schiff-base ligand), have been synthesized by reacting [$RuHCl(CO)(PPh_3)_3$], [$RuHCl(CO)(AsPh_3)_3$], and [$RuHCl(CO)(Py)(PPh_3)_2$] with the Schiff base in 1 : 1 molar ratio in an ethanol–benzene mixture. These complexes have been characterized by elemental analysis, FT-IR, UV-Vis, NMR, and mass spectroscopy. The redox behaviors of the complexes have been investigated by cyclic voltammetry. These complexes have been examined for their catalytic efficiency for aryl–aryl coupling and oxidation of primary and secondary alcohols into their corresponding aldehydes and ketones in the presence of oxygen. All the complexes were screened for their antibacterial activity. Further, one complex was tested for its binding with calf thymus-DNA using absorption spectroscopic studies and viscosity measurements.

Keywords: Thiosemicarbazone; Molecular oxygen; Aryl–aryl coupling; Antibacterial; DNA-binding

1. Introduction

Thiosemicarbazones are an important class of N, S donors which have pharmacological interest due to their significant antibacterial, antiviral, antimalarial, antileprotic, and anticancer activities [1–8]. Thiosemicarbazones usually are chelating ligands with transition metal ions, bonding through sulfur and hydrazine nitrogen [9–11]. The chemistry of ruthenium receives attention primarily because of the fascinating electron-transfer and energy-transfer properties displayed by the complexes of this metal [12]. Ruthenium offers a wide range of oxidation states and reactivity of the ruthenium complexes depend on the stability and interconvertibility of these oxidation states, which in turn depend on the nature of the ligands bound to the metal. Transition metal complexes are effective catalysts in cross-coupling reactions, but their use as catalysts for aryl–aryl coupling has not been much studied. Mild and efficient aromatic couplings have been reported [13]. Selective oxidation of alcohols to aldehydes and ketones is a

*Corresponding author. Email: cjayabalakrishnan@gmail.com

Journal of Coordination Chemistry
ISSN 0095-8972 print/ISSN 1029-0389 online © 2011 Taylor & Francis
DOI: 10.1080/00958972.2011.556721

key reaction in organic synthesis. The development of new procedures that can use air or molecular oxygen as oxidant is environmentally attractive [14]. Research has described the use of solid-supported heterogeneous catalysts, notably ruthenium-based for the aerobic oxidation of alcohols [15]. DNA-binding metal complexes have been extensively studied as DNA structural probes, DNA-dependent electron-transfer probes, DNA foot printing and sequence-specific cleaving agents, and potential anticancer drugs [16–18].

Here we report the synthesis, characterization, catalytic, biological, and DNA-binding activities of Ru(II) complexes containing triphenylphosphine/arsine/pyridine as coligands. Mixed-chelate complexes of ruthenium have been synthesized using tetradentate Schiff-base ligands derived by the condensation of salicylaldehyde/*o*-hydroxyacetophenone/*o*-vanillin/2-hydroxy-1-naphthaldehyde with thiosemicarbazide and furfuraldehyde (scheme 1).

2. Experimental

2.1. *Materials and measurements*

All reagents used were of analar grade. Solvents were purified and dried according to the literature procedures [19]. $RuCl_3 \cdot 3H_2O$ was purchased from Loba Chemie and used without purification. The starting complexes $[RuHCl(CO)(PPh_3)_3]$ [20], $[RuHCl(CO)(AsPh_3)_3]$ [21], and $[RuHCl(CO)(Py)(PPh_3)_2]$ [22] were prepared by literature methods. Microanalyses were performed at Sophisticated Test and Instrumentation Centre (STIC), Cochin University of Science and Technology, Kerala. Infrared (IR) spectra were recorded using KBr pellets on a Perkin-Elmer

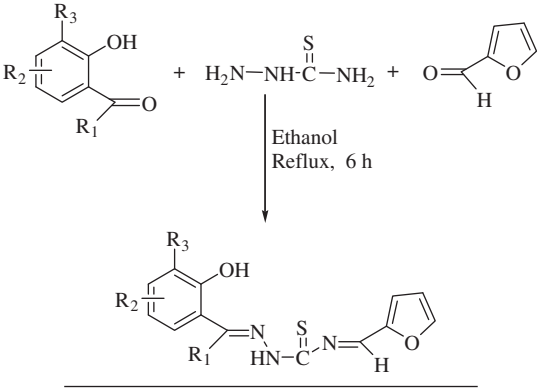

R_1	R_2	R_3	Abbreviation
H	H	H	H_2L^1
CH_3	H	H	H_2L^2
H	H	OCH_3	H_2L^3
H	C_4H_4	H	H_2L^4

Scheme 1. Formation of Schiff-base ligands.

FT-IR 8000 spectrometer RX1 model from 4000 to 400 cm^{-1}. Electronic spectra of the complexes were recorded in dichloromethane with a Systronics-2202 double beam spectrophotometer from 800 to 200 nm. The ^{1}H- and ^{13}C-NMR spectra of the ligands and complexes were recorded with a Bruker WM 500 DCX MHz instrument using TMS as an internal standard. ^{31}P NMR spectra were recorded with a Bruker WM 500 DCX MHz instrument using orthophosphoric acid as an internal standard. Mass spectra were recorded with a JEOL GC make instrument at Indian Institute of Technology, Chennai. Cyclic voltammetric studies were carried out on a CHN Instrument in dichloromethane using a glassy carbon working electrode. A platinum electrode and a saturated calomel electrode were used as counter and reference electrodes, respectively. Melting points were recorded with a Veego DS Model apparatus and are uncorrected.

2.2. *Preparation of dibasic tetradentate Schiff bases*

To an ethanolic solution of salicylaldehyde/*o*-hydroxyacetophenone/*o*-vanilin/2-hydroxy-1-naphthaldehyde (20 mmol), thiosemicarbazide (20 mmol) and furfuraldehyde (20 mmol) were added and stirred along with a few drops of glacial acetic acid. The mixture was then refluxed for 6 h. On cooling, a solid separated out and was recrystallized from ethanol. The purity of the ligand was checked by thin layer chromatography (TLC).

2.3. *Preparation of ruthenium(II) Schiff-base complexes*

The Schiff bases (H_2L^1–H_2L^4) (0.1 mmol) were added to a solution of [RuHCl(CO)(EPh_3)$_2$B] (where E = P/As, B = PPh_3/$AsPh_3$/Py) (0.1 mmol) in 1 : 1 molar ratio in ethanol–benzene (1 : 1) and the mixture was refluxed for 6 h. The resulting solution was concentrated to about 3 cm^3 and the complexes were precipitated by the addition of a small quantity of petroleum ether (60–80°C). The complexes were then filtered, washed with petroleum ether and recrystallized from CH_2Cl_2/petroleum ether, and dried under vacuum (scheme 2).

2.4. *Catalytic oxidation experiments*

A solution of alcohol (0.1 mL, 1 mmol) in dichloromethane (20 mL) was added to a solution of the free ligands, metal precursors, and ruthenium(II) complex (0.01 mmol) and stirred for 6 h under oxygen at ambient temperature. The mixture was evaporated to dryness and extracted with petroleum ether (60–80°C). The combined petroleum ether extracts were filtered and evaporated to give the corresponding carbonyl compound which was then quantified as their 2,4-dinitrophenyl hydrazones [23].

2.5. *Aryl–aryl coupling experiments*

Magnesium turnings (0.320 g) were placed in a flask equipped with a $CaCl_2$ guard tube. A crystal of iodine was added. PhBr [0.75 cm^3 of total 1.88 cm^3] in anhydrous Et_2O (5 cm^3) was added dropwise and the mixture was refluxed for 40 min. To this mixture,

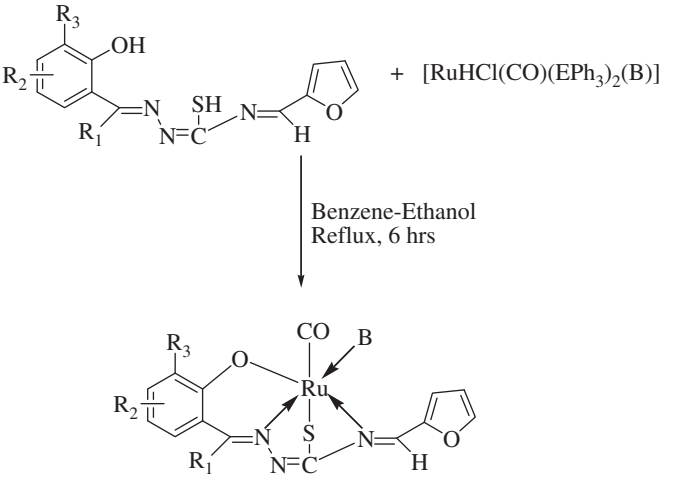

where $R_1 = H/CH_3$; $R_2 = H/C_4H_4$; $R_3 = H/OCH_3$; E = P/As; B = $PPh_3/AsPh_3$/Py

Scheme 2. Formation of ruthenium(II) Schiff-base complexes.

1.03 cm^3 (0.01 mol) of PhBr in anhydrous Et_2O (5 cm^3) and the free ligands, metal precursors, and ruthenium complex (0.05 mmol) chosen for investigation were added and heated under reflux for 6 h. The reaction mixture was cooled and hydrolyzed with a saturated solution of aqueous NH_4Cl and the ether extract on evaporation gave a crude product of biphenyl which was chromatographed to get pure biphenyl, which was compared with an authentic sample (m.p. 69–72°C) [24].

2.6. *Antibacterial activities*

Solvent, free ligands, metal precursors, and new ruthenium(II) complexes were tested *in vitro* for their effect on certain human pathogenic bacteria by the Kirby Bauer method [25]. The ligands, metal precursor complexes, and their ruthenium(II) complexes were stored dry at room temperature and dissolved in dichloromethane. Both the Gram positive (*Staphylococcus aureus*) and Gram negative (*Escherichia coli*) bacteria were grown in Muller Hinton agar medium and incubated at 37°C for 24 h followed by frequent substrate to fresh medium and were inoculated with a loop full of bacterial culture and spread throughout the petriplates uniformly with a sterile glass spreader. To each disc, the test samples and reference antibiotic (amikacin) were added with a sterile micropipette. The plates were then incubated at 35 ± 2°C for 24 h for bacteria. Plates containing respective solvents served as control. Inhibition was recorded by measuring the diameter of the inhibitory zone after incubation.

2.7. *DNA-binding experiments*

All experiments were carried out in buffer (5 mm Tris-HCl, 50 mm NaCl, pH 7.2) at room temperature. A solution of calf-thymus DNA (CT-DNA) in buffer gave a ratio of

Table 1. Analytical data of the ligands and complexes.

Ligand/complex	Color	Mol. mass	Calculated (found) (%)			
			C	H	N	S
H_2L^1	Brown	273	57.13(57.02)	4.06(4.34)	15.37(15.90)	11.73(11.21)
H_2L^2	Brown	287	58.52(58.96)	4.56(4.23)	14.62(14.30)	11.16(11.72)
H_2L^3	Sandal	303	55.43(55.10)	4.32(4.58)	13.85(13.16)	10.57(10.98)
H_2L^4	Yellow	323	63.14(63.72)	4.05(4.52)	12.99(12.72)	9.92(9.16)
$[RuCO(PPh_3)L^1]$	Yellow	663	58.00(58.36)	3.65(3.23)	6.34(6.48)	4.84(4.32)
$[RuCO(PPh_3)L^2]$	Yellow	677	58.57(58.93)	3.87(3.61)	6.21(6.78)	4.74(4.52)
$[RuCO(PPh_3)L^3]$	Yellow	693	57.22(57.73)	3.78(3.21)	6.07(6.72)	4.63(4.41)
$[RuCO(PPh_3)L^4]$	Yellow	713	60.67(60.12)	3.68(3.41)	5.90(5.60)	4.50(4.22)
$[RuCO(AsPh_3)L^1]$	Yellow	707	54.39(54.76)	3.42(3.93)	5.95(5.73)	4.54(4.03)
$[RuCO(AsPh_3)L^2]$	Yellow	721	55.00(55.41)	3.64(3.41)	5.83(5.61)	4.45(4.21)
$[RuCO(AsPh_3)L^3]$	Yellow	737	53.81(53.23)	3.56(3.12)	5.70(5.45)	4.35(4.12)
$[RuCO(AsPh_3)L^4]$	Yellow	757	57.14(57.73)	3.46(3.66)	5.55(5.21)	4.24(4.71)
$[RuCO(Py)L^1]$	Yellow	480	47.59(46.90)	2.94(2.53)	11.69(12.81)	6.69(6.21)
$[RuCO(Py)L^2]$	Yellow	494	48.68(48.47)	3.27(3.30)	11.35(11.81)	6.50(6.13)
$[RuCO(Py)L^3]$	Yellow	510	47.15(45.61)	3.17(3.72)	11.00(11.71)	6.29(6.91)
$[RuCO(Py)L^4]$	Yellow	530	52.17(51.91)	3.05(2.83)	10.58(10.16)	6.06(6.59)

UV absorbances at 260 and 280 nm of *ca* 1.8–1.9 : 1, indicating that the DNA was sufficiently free of protein [26]. The concentration of CT-DNA per nucleotide was determined spectrophotometrically ($\varepsilon_{260} = 6600\,(\text{mol L}^{-1})^{-1}\,\text{cm}^{-1}$) [27]. Stock solutions were stored at 4°C and used within 3 days. Titration experiments were performed at a fixed complex concentration (20 μm), to which CT-DNA stock solution was added up to a [DNA]/[Ru] ratio of 1 : 1. The mixture was allowed to equilibrate for 5 min before spectra were recorded.

2.8. *Viscosity measurements*

For viscosity measurements, the Ubbelohde viscometer was thermostated at 25°C in a constant temperature bath. The concentration of DNA was 160 μm in NP and the flow-times were determined with a digital timer ($1/R = [\text{Ru}]/[\text{DNA}] = 0.5$).

3. Results and discussion

Light- and air-stable ruthenium(II) complexes [Ru(CO)(B)(L)] [B = PPh_3/$AsPh_3$ or pyridine (py); L = dibasic tetradentate Schiff-base ligand] have been prepared by reacting $[RuHCl(CO)(EPh_3)_2(B)]$, where E = P/As; B = PPh_3/PPh_3/Py with the respective Schiff bases in a 1 : 1 molar ratio in benzene–ethanol mixture. The analytical data (table 1) for the complexes agree well with the proposed molecular formulae. In all reactions, the Schiff bases are binegative tetradendate ligands.

3.1. *Spectroscopic studies*

3.1.1. FT-IR spectra. FT-IR spectra of the free ligands were compared with those of the new complexes to confirm coordination of ligand to ruthenium (table 2). The ligand

Table 2. IR and electronic spectroscopic data of the ligands and complexes.

Ligand/complex	FT-IR (cm^{-1})				UV-Vis	
	$\nu_{-C=N-}$	ν_{Ph-C-O}	ν_{-C-S}	ν_{Py}	λ_{max} (nm)	ε_{max} ($dm^3\,mol^{-1}\,cm^{-1}$)
H_2L^1	1625	1266	–	–	303, 368	395, 498
H_2L^2	1630	1277	–	–	305, 363	528, 650
H_2L^3	1620	1263	–	–	308, 368	349, 441
H_2L^4	1628	1277	–	–	305, 370, 406	315, 397, 467
$[RuCO(PPh_3)L^1]$	1603	1290	746	–	254, 355	3190, 3380
$[RuCO(PPh_3)L^2]$	1609	1329	745	–	252, 356	3168, 3395
$[RuCO(PPh_3)L^3]$	1602	1320	743	–	252, 294, 363	1042, 1063, 1224
$[RuCO(PPh_3)L^4]$	1614	1310	744	–	253, 294, 382, 484	792, 369, 539, 173
$[RuCO(AsPh_3)L^1]$	1602	1306	737	–	258, 347, 450	827, 425, 103
$[RuCO(AsPh_3)L^2]$	1619	1282	741	–	252, 314, 342	1341, 1375, 1390
$[RuCO(AsPh_3)L^3]$	1601	1310	737	–	253, 301, 349, 442	1600, 1519, 1499, 478
$[RuCO(AsPh_3)L^4]$	1615	1357	737	–	254, 334, 373, 383, 460	1058, 808, 716, 318, 100
$[RuCO(Py)L^1]$	1602	1302	746	1030	254, 294, 362, 456	3618, 3163, 3085, 738
$[RuCO(Py)L^2]$	1600	1305	738	1027	254, 301, 357	1731, 1565, 1543
$[RuCO(Py)L^3]$	1600	1315	744	1025	254, 293, 362, 456	727, 641, 628, 115
$[RuCO(Py)L^4]$	1614	1298	744	1032	253, 286, 373, 392, 472	648, 634, 622, 581, 194

can exhibit thione–thiol tautomerism. The FT-IR spectra of the free ligands showed a band at 1620–1630 cm^{-1} characteristic of the azomethine group (>C=N), whereas in complexes this band is slightly shifted to lower frequency at 1600–1619 cm^{-1}. This indicates coordination of the Schiff bases through the azomethine nitrogen [28]. The band of medium intensity at 1059–1061 cm^{-1} in all ligands may be assigned to C=S stretch. In spectra of the complexes, this band disappears and a new band appears at 737–746 cm^{-1}, attributed to enolization of the –NH–C=S group and subsequent coordination through deprotonated sulfur [29]. For the ligands, strong bands at 681–705 cm^{-1} are due to the furan ring. On complexation, there is no change in the furan ring owing to the non-involvement of the hetero atom in coordination. A strong band due to phenolic C–O was observed at 1263–1277 cm^{-1} in the ligands, shifted to higher frequency (1282–1357 cm^{-1}) in the complexes, showing that the other coordination site was through the phenolic oxygen [30–32]. This was further supported by the disappearance of the broad band at 3219 cm^{-1} due to phenolic OH in the complexes. For all the complexes, IR spectra showed a strong band at 1930–1952 cm^{-1} due to a terminally coordinated carbonyl. For $[Ru(CO)(Py)(L^1)]$, $[Ru(CO)(Py)(L^2)]$, $[Ru(CO)(Py)(L^3)]$, and $[Ru(CO)(Py)(L^4)]$, IR spectra showed a medium intensity band at 1025–1032 cm^{-1} characteristic of coordinated nitrogen base [22]. Characteristic bands for triphenylphosphine/arsine were also present in the expected region 1428–1435 cm^{-1} [33].

3.1.2. Electronic spectra. Electronic absorption spectra of the free ligands and their complexes in CH_2Cl_2 are listed in table 2. Spectra of all the free ligands showed two types of transition at 303–308 and 363–406 nm due to π–π^* and n–π^* transitions involving the benzene ring, –C=N, and enolic S–H. These bands were shifted in spectra of the complexes, indicating the involvement of imine group nitrogen and thionyl sulfur in coordination with the central metal. Spectra of the complexes showed three to four

Table 3. ^{1}H-NMR data of ligands and Ru(II) Schiff-base complexes.

Ligand/complex	^{1}H-NMR spectra
H_2L^1	6.6–8.2 (Ar, m), 8.4 (H–C=N, s), 11.3 (SH, s), 9.9 (Ph–OH, s)
H_2L^2	6.5–8.0 (Ar, m), 8.6 (H–C=N, s), 11.9 (SH, s), 10.5 (Ph–OH, s), 1.9 (–CH_3–C=N, s)
H_2L^3	6.8–7.9 (Ar, m), 8.4 (H–C=N, s), 11.4 (SH, s), 9.2 (Ph–OH, s), 3.8 (–OCH_3, s)
H_2L^4	7.2–8.6 (Ar, m), 9.0 (H–C=N, s), 11.4 (SH, s), 10.5 (Ph–OH, s)
[RuCO(PPh_3)L^1]	6.5–7.9 (Ar, m), 8.4 (H–C=N, s)
[RuCO(PPh_3)L^2]	6.5–7.8 (Ar, m), 8.4 (H–C=N, s), 2.0 (–CH_3–C=N, s)
[RuCO(PPh_3)L^3]	6.9–7.7 (Ar, m), 8.5 (H–C=N, s), 3.7 (–OCH_3, s)
[RuCO(PPh_3)L^4]	6.6–8.3 (Ar, m), 8.8 (H–C=N, s)
[RuCO($AsPh_3$)L^1]	6.5–7.9 (Ar, m), 8.1 (H–C=N, s)
[RuCO($AsPh_3$)L^2]	6.6–8.0 (Ar, m), 8.5 (H–C=N, s), 2.0 (–CH_3–C=N, s)
[RuCO($AsPh_3$)L^3]	6.9–7.9 (Ar, m), 8.4 (H–C=N, s), 3.5 (–OCH_3, s)
[RuCO($AsPh_3$)L^4]	6.9–8.6 (Ar, m), 9.1 (H–C=N, s)
[RuCO(Py)L^1]	7.7–8.0 (Ar, m), 8.3 (H–C=N, s)
[RuCO(Py)L^2]	6.6–7.9 (Ar, m), 8.3 (H–C=N, s), 2.0 (–CH_3–C=N, s)
[RuCO(Py)L^3]	6.6–7.8 (Ar, m), 8.4 (H–C=N, s), 3.5 (–OCH_3, s)
[RuCO(Py)L^4]	6.6–8.3 (Ar, m), 9.1 (H–C=N, s)

bands at 252–484 nm. All Schiff-base ruthenium complexes were diamagnetic, indicating the presence of ruthenium(II). The ground state of ruthenium(II) in an octahedral environment is $^1A_{1g}$ and the excited states corresponding to $t_{2g}^5e_g^1$ configuration are $^3T_{1g}$, $^3T_{2g}$, $^1T_{1g}$, and $^1T_{2g}$. Hence, four bands corresponding to the transitions $^1A_{1g} \rightarrow {}^3T_{1g}$, $^1A_{1g} \rightarrow {}^3T_{2g}$, $^1A_{1g} \rightarrow {}^1T_{1g}$, and $^1A_{1g} \rightarrow {}^1T_{2g}$ are possible in the order of increasing energy. The high-intensity bands at 252–349 nm were characterized as ligand-centered bands, designated as π–π^* and n–π^* transitions for electrons localized on the azomethine of the Schiff base. The band at 355–484 nm has been assigned to the spin-allowed $^1A_{1g} \rightarrow {}^1T_{1g}$ transition, based on the low-extinction coefficient values (ε) as compared to charge-transfer bands [34–37]. The pattern of the electronic spectra for the complexes indicates the presence of an octahedral environment around the ruthenium(II) similar to other ruthenium octahedral complexes [30, 34, 36, 37].

3.1.3. ^{1}H-NMR spectra. ^{1}H-NMR spectra of ligands and complexes were recorded in DMSO-d_6 to confirm the binding mode of the Schiff base to ruthenium ion; the values are given in table 3 (Supplementary material). Aromatic protons for the ligands appear as multiplets at 6.5–8.6 ppm. The H–C=N, –SH, and Ph–OH protons appear as singlets at 8.4–9.0, 11.3–11.9, and 9.2–10.5 ppm for all the Schiff bases. In H_2L^2, the azomethine methyl protons are a singlet at 1.9 ppm. The methoxy protons of H_2L^3 are a singlet at 3.8 ppm. On complexation, a multiplet at 6.5–8.6 ppm is assigned to aromatic protons, triphenylphosphine/arsine, and pyridine protons. The azomethine proton signals in the complexes are at 8.1–9.1 ppm, shifted on complexation indicating coordination through the azomethine nitrogen to metal ion. The azomethine methyl protons are a singlet at 2.0 ppm for [Ru(CO)(PPh_3)L^2], [Ru(CO)($AsPh_3$)L^2], and [Ru(CO)(Py)L^2], while methoxy protons of [Ru(CO)(PPh_3)L^3], [Ru(CO)($AsPh_3$)L^3], and [Ru(CO)(Py)L^3] are a singlet at 3.5–3.7 ppm. The absence of Ph–OH and –SH resonance in the complexes indicates the deprotonation of phenol and thiol of the Schiff base on complexation and coordination to ruthenium through phenolic oxygen and thiolic sulfur.

Table 4. ^{13}C-NMR spectra of Ru(II) Schiff-base complexes.

Ligand/complex	^{13}C-NMR spectra
H_2L^1	112–132 (Ar, C), 140 (C–S), 156.2 (C=N)
H_2L^2	114–125 (Ar, C), 131 (C–S), 150 (C=N), 19(CH_3)
H_2L^3	112–121 (Ar, C), 139 (C–S), 148 (C=N), 56 (–OCH_3)
H_2L^4	118–132 (Ar, C), 143 (C–S), 157 (C=N)
[Ru(CO)(PPh_3)(L^4)]	128–134 (Ar, C), 123 (C–S), 144 (C=N), 180(C≡O)
[Ru(CO)($AsPh_3$)(L^1)]	126–135 (Ar, C), 126 (C–S), 140 (C=N), 177(C≡O)
[Ru(CO)($AsPh_3$)(L^2)]	128–133 (Ar, C), 126 (C–S), 135 (C=N), 19(CH_3), 175(C≡O)
[RuCO(Py)L^3]	128–134 (Ar, C), 123 (C–S), 148 (C=N), 55 (–OCH_3), 180(C≡O)

3.1.4. ^{13}C-NMR spectra. ^{13}C-NMR data were recorded in $CDCl_3$ solution and the assignments of ligands and complexes are listed in table 4 (Supplementary material). ^{13}C-NMR spectra of H_2L^1–H_2L^4 display a single resonance at 148–157 ppm for azomethine carbons, which confirms the structure of ligands. The thiolic carbon of the Schiff bases appeared at 131–143 ppm. The signal due to the methyl carbon of H_2L^2 and methoxy carbon of H_2L^3 appear at 19 and 56 ppm, respectively. The aromatic carbons for all the ligands appear at 112–132 ppm. For [Ru(CO)(PPh_3)L^4], [Ru(CO)($AsPh_3$)L^1], [Ru(CO)($AsPh_3$)L^2], and [Ru(CO)(Py)L^3], aromatic carbons appear at 126–135 ppm. The thiolic carbon and azomethine carbons appear at 123–126 and 135–148 ppm [38], respectively. The signals due to methyl carbon of [Ru(CO)($AsPh_3$)L^2] and methoxy carbon of [Ru(CO)(Py)L^3] appear at 19 and 55 ppm, respectively. For all complexes, the terminal carbonyl group appears at 175–180 ppm [39].

3.1.5. ^{31}P-NMR spectra. ^{31}P-NMR spectra were recorded for two complexes to confirm the presence of triphenylphosphine and to determine the geometry of the complexes. [Ru(CO)(PPh_3)L^4] has one signal at 28.62 ppm, confirming the presence of only one triphenylphosphine.

3.1.6. Mass spectra. The mass spectrum of [RuCO(Py)L^2] was recorded and the appearance of molecular ion peak at 493.65 confirms the proposed molecular formula of the complex. The mass spectrum of the complex is shown in Supplementary material.

3.2. Electrochemical study

Electrochemical properties of all the complexes were studied in dichloromethane solution by cyclic voltammetry and voltammetric data are presented in table 5. Cyclic voltammograms of all the complexes exhibit a quasireversible oxidation and an irreversible reduction at scan rate of 100 mV s^{-1}. Representative cyclic voltammogram of [Ru(CO)(PPh_3)L^3] is shown in Supplementary material. In Ru(III)–Ru(II) couple, the complexes [Ru(CO)(PPh_3)L^1], [Ru(CO)(PPh_3)L^4], and [Ru(CO)(PPh_3)L^1] are irreversible and [Ru(CO)($AsPh_3$)L^2] and [Ru(CO)(Py)L^1] are reversible, while the remaining complexes are quasireversible [40] with peak to peak separation (ΔE_p) of 130–740 mV. This is attributed to slow electron transfer and adsorption of the

Table 5. Cyclic voltammetry data of the Ru(II) Schiff-base complexes.[a]

	Ru^{III}–Ru^{II}				Ru^{II}–Ru^{I}			
Complex	E_{pc} (V)	E_{pa} (V)	E_f (V)	ΔE_P (mV)	E_{pc} (V)	E_{pa} (V)	E_f (V)	ΔE_P (mV)
$[RuCO(PPh_3)L^1]$	–	0.82	–	–	−0.71	–	–	–
$[RuCO(PPh_3)L^2]$	0.44	0.82	0.63	380	–	–	–	–
$[RuCO(PPh_3)L^3]$	0.50	1.22	1.11	720	−0.81	–	–	–
$[RuCO(PPh_3)L^4]$	–	0.84	–	–	−0.63	–	–	–
$[RuCO(AsPh_3)L^1]$	0.94	–	–	–	–	−0.79	–	–
$[RuCO(AsPh_3)L^2]$	0.91	0.99	0.95	80	−0.30	–	–	–
$[RuCO(AsPh_3)L^3]$	0.30	0.84	0.57	540	–	–	–	–
$[RuCO(AsPh_3)L^4]$	0.27	1.01	0.64	740	–	–	–	–
$[RuCO(Py)L^1]$	0.91	0.81	0.86	100	−0.85	–	–	–
$[RuCO(Py)L^2]$	0.87	0.74	0.81	130	−0.82	–	–	–
$[RuCO(Py)L^3]$	0.69	1.18	0.94	490	−0.12	−0.73	−0.43	610
$[RuCO(Py)L^4]$	0.94	0.67	0.81	270	−0.16	–	–	–

[a]Supporting electrolyte $[NBu_4]ClO_4$ (0.1 mol L^{-1}); all potentials are referenced to Ag/AgCl; $E_f = 0.5(E_{pa} + E_{pc})$, where E_{pa} and E_{pc} are anodic and cathodic peak potentials, respectively; scan rate, 100 mV s^{-1}.

complexes on to the electrode surface [41]. The reason for the irreversibility observed for the reductive response of the complexes may be due to a short-lived reduced state of the metal ion or due to the oxidative degradation of the ligands [42]. The different redox behavior of the complexes can be accredited to the different substituents present in the thiosemicarbazone ligands [43]. From the electrochemical data, the present system stabilizes the higher oxidation state of ruthenium.

3.3. *Catalytic activity studies*

3.3.1. Oxidation of alcohols. Activation of molecular oxygen by transition metals for catalytic oxidation of organic substrates is of interest in organic synthesis [44, 45]. Catalytic oxidation of primary and secondary alcohols by free ligands, metal precursors, and ruthenium(II) Schiff-base complexes were carried out in CH_2Cl_2 under oxygen at room temperature; the results are summarized in table 6 for benzylalcohol, cyclohexanol, propane-1-ol, and butane-1-ol. After stirring for 6 h the resulting carbonyl compounds were quantified as 2,4-dinitrophenyl hydrazone derivatives by gravimetric estimation. Without the catalyst, only a very small amount of carbonyl compound is formed during oxidation, which is insignificant compared with the yields of carbonyl compounds obtained from reactions catalyzed by free ligands, metal precursors, and ruthenium complexes. The precursor complexes have higher activity than free ligands but lower than the newly synthesized complexes. All the new complexes catalyze the oxidation of alcohol to aldehyde or ketone, but the yields and turnover vary with different catalysts. Compared to other metal complexes, ruthenium complexes have better catalytic activities for catalytic oxidation [44]. Catalytic efficiencies of complexes derived from salicylaldehyde, 2-hydroxy-1-naphthaldehyde, and amines were lower than those derived from *o*-hydroxyacetophenone and *o*-vanillin. The essential difference between these complexes is that the hydrogen of the aldehyde of salicylaldehyde and 2-hydroxy-1-naphthaldehyde is replaced by the electron-donating methyl in *o*-hydroxyacetophenone and methoxy group in *o*-vanillin. Thus, it seems that

Table 6. Catalytic activity data.

Metal precursors, ligands and complexes	Aryl-aryl coupling reaction			Oxidation of alcohols						
	Biphenyl			Benzylalcohol → Benzaldehyde		Cyclohexanol → Cyclohexanone		Propane-1-ol → Propionaldehyde		Butane-1-ol → Butanaldehyde	
	mg	Yield (%)	Yield (%)	Turnover number[a]	Yield (%)	Turnover number[a]	Yield (%)	Turnover number[a]	Yield (%)	Turnover number[a]
$[RuHCl(CO)(PPh_3)_3]$	0.108	11.22	21.9	22.7	19.2	20.0	16.1	21.4	18.6	20.6
$[RuHCl(CO)(AsPh_3)_3]$	0.105	10.91	21.2	22.0	18.2	18.9	15.1	20.1	17.5	19.4
$[RuHCl(CO)(Py)(PPh_3)_2]$	0.100	10.39	20.2	20.9	17.5	18.2	14.1	18.7	16.3	18.0
H_2L^1	0.097	9.34	17.9	18.2	16.3	17.1	11.3	14.98	14.3	15.8
H_2L^2	0.103	9.91	19.7	20.6	17.3	18.1	14.0	15.9	15.8	17.5
H_2L^3	0.101	9.72	18.6	19.4	16.6	17.4	12.8	16.9	14.9	16.5
H_2L^4	0.092	8.85	17.5	18.2	15.7	16.4	11.6	15.4	12.3	13.6
$[RuCO(PPh_3)L^1]$	0.242	23.29	61.73	64.47	57.90	60.50	44.3	58.9	49.88	55.34
$[RuCO(PPh_3)L^2]$	0.396	38.11	79.5	83.08	67.55	70.55	46.63	62.08	52.7	58.5
$[RuCO(PPh_3)L^3]$	0.440	42.35	66.5	69.5	65.36	68.27	44.6	59.4	51.00	56.5
$[RuCO(PPh_3)L^4]$	0.239	23.00	60.36	68.27	56.91	59.44	42.88	57.09	47.00	52.15
$[RuCO(AsPh_3)L^1]$	0.443	42.63	63.82	66.65	56.90	59.44	45.25	60.25	48.13	53.40
$[RuCO(AsPh_3)L^2]$	0.533	51.30	71.73	74.93	66.80	69.12	45.63	60.75	50.25	55.76
$[RuCO(AsPh_3)L^3]$	0.498	47.93	67.73	70.74	65.46	68.36	46.25	61.59	52.00	57.7
$[RuCO(AsPh_3)L^4]$	0.396	38.11	60.73	63.43	51.91	54.22	42.50	56.59	46.2	51.32
$[RuCO(Py)L^1]$	0.218	20.98	64.82	67.70	58.91	61.53	43.25	57.59	49.13	54.51
$[RuCO(Py)L^2]$	0.421	40.52	69.73	72.83	67.91	70.93	46.88	62.42	51.25	56.87
$[RuCO(Py)L^3]$	0.309	29.74	62.64	65.42	61.36	64.09	44.25	58.92	50.63	56.18
$[RuCO(Py)L^4]$	0.297	28.58	64.81	67.70	42.82	44.72	43.25	57.59	48.75	54.96

[a]Moles of product per mole of catalyst.

the presence of electron-donating methyl and methoxy enhances the catalytic activity of acetophenone and *o*-vanillin complexes over the other two, in agreement with earlier observations [46]. However, there is a report in which the catalytic activity is increased by electron-donating substituent [47, 48]. The relatively higher product yield obtained for the oxidation of benzyl alcohol compared with the other alcohols is because the α-CH of benzyl alcohol is more acidic than cyclohexanol, 1-propanol, and butane-1-ol [49].

3.3.2. Aryl–aryl coupling reaction. The free ligands, metal precursors, and new ruthenium(II) complexes have been used as catalysts for phenyl–phenyl coupling; the results are summarized in table 6. The system chosen for study is the coupling of phenyl magnesium bromide with bromobenzene to give biphenyl as product. Bromobenzene was first converted into the corresponding Grignard reagent. Then bromobenzene followed by the ligands and the complex chosen for investigations was added to the above reagent and the mixture was heated under reflux for 6 h. After 6 h, the mixture yielded biphenyl, which was compared with an authentic sample. Only a very small amount of biphenyl was isolated when the reaction was carried out without the catalyst [30]. The yield of biphenyl, obtained from the reaction catalyzed by the new ruthenium(II) complexes, are low when compared to the yield obtained from reactions catalyzed by $[NiCl_2(PPh_3)_2]$. This may be due to the active species derived from ruthenium complexes being less stable than the active species from $[NiCl_2(PPh_3)_2]$, as the effectiveness of the catalysts is directly related to their ability to generate the corresponding active species [24].

3.4. *Antibacterial activity*

The free ligands, metal precursors, and Schiff-base complexes were screened *in vitro* for their antibacterial activity against certain pathogenic bacteria at four different concentrations using the Kirby Bauer method [25]. These compounds exhibit considerable activity against Gram positive (*S. aureus*) and Gram negative (*E. coli*) bacteria. Test solutions were prepared in dichloromethane and the results are summarized in table 7. Ruthenium chelates possess higher antibacterial activity than the respective free ligands and metal precursors against the same bacteria, suggesting that chelation facilitates the ability of a complex to cross a cell membrane [50–53]. Furthermore, the mode of action of the compounds may involve the hydrogen bond through >C=N group with active centers of all cell constituents resulting in interference with normal cell process [53]. The *o*-hydroxyacetophenone Schiff-base complex showed more activity than salicylaldehyde Schiff-base complex due to the presence of more electron-donating ($-CH_3$) group in these complexes [54]. The present results show that the ruthenium(II) carbonyl Schiff-base complexes possess better cytotoxicity than other metal complexes against the same bacteria [55]. Although the complexes were active, they did not reach the effectiveness of the conventional bacteriocide amikacin.

3.5. *DNA-binding studies – adsorption spectroscopic studies*

DNA binding of $[RuCO(PPh_3)L^2]$ was determined by following the changes in the absorbance and shift in wavelength on each addition of DNA solution to the complex.

Table 7. Antibacterial studies of metal precursors, ligands and Ru(II) Schiff-base complexes.

Ligands, metal precursors and complexes	Diameter of inhibition zone (mm)							
	S. aureus				*E. coli*			
	0.5%	1.0%	1.5%	2.0%	0.5%	1.0%	1.5%	2.0%
$[RuHCl(CO)(PPh_3)_3]$	–	5	7	9	2	5	6	6
$[RuHCl(CO)(AsPh_3)_3]$	3	5	9	9	4	7	7	8
$[RuHCl(CO)(Py)(PPh_3)_2]$	5	6	7	10	5	7	9	11
H^2L^1	5	12	18	23	–	13	5	8
H^2L^2	8	14	23	29	–	–	5	10
H^2L^3	10	15	19	28	4	7	12	14
H^2L^4	12	17	21	25	3	8	15	21
$[RuCO(PPh_3)L^1]$	10	13	18	25	5	10	14	20
$[RuCO(PPh_3)L^2]$	15	21	30	32	6	12	16	20
$[RuCO(PPh_3)L^3]$	10	17	25	28	8	14	20	28
$[RuCO(PPh_3)L^4]$	5	8	18	23	–	–	–	–
$[RuCO(AsPh_3)L^1]$	8	15	19	23	5	9	14	23
$[RuCO(AsPh_3)L^2]$	12	19	25	31	8	14	21	29
$[RuCO(AsPh_3)L^3]$	10	17	23	29	9	15	24	31
$[RuCO(AsPh_3)L^4]$	7	13	18	23	10	18	26	32
$[RuCO(Py)L^1]$	7	13	18	26	12	20	20	35
$[RuCO(Py)L^2]$	13	20	25	30	8	15	21	29
$[RuCO(Py)L^3]$	10	18	25	29	9	13	21	27
$[RuCO(Py)L^4]$	–	–	–	–	9	14	20	26
Amikacin	20	22	23	26	19	21	23	26

A representative absorption spectrum is given in figure 1. In the figure, the blank represents the absorption spectra without DNA and 5, 10, 15, and 20 mmol represents the concentration of the CT-DNA. The ruthenium(II) complex in DMSO buffer mixture exhibits an intense transition around 360–310 nm, which is attributed to a $\pi \rightarrow \pi^*$ intraligand transition. On titration of CT-DNA with the complex, considerable increase or decrease in the absorption along with small red or blue shift was observed. The titration process was repeated until no further change was observed in the spectrum. The complex exhibits 52% hypochromicity and 2 nm bathochromism in the presence of DNA at saturation. During the titration, the extent of hypochromicity and bathochromism varied, implying binding of the complex to DNA through different modes [56]; the hypochromism confirms strong binding of the complex to DNA.

3.6. *Viscosity measurements*

Viscosity measurements which are sensitive to length change are regarded as the most critical tests for binding mode. Changes in relative viscosity provide a reliable method for distinguishing between intercalators and electrostatic binders of DNA. The effect of $[RuCO(PPh_3)L^2]$ on the viscosity of CT-DNA is shown in figure 2. With the increasing amounts of the complex, the viscosity of DNA increases steadily showing that the complex binds to CT-DNA through intercalation [56].

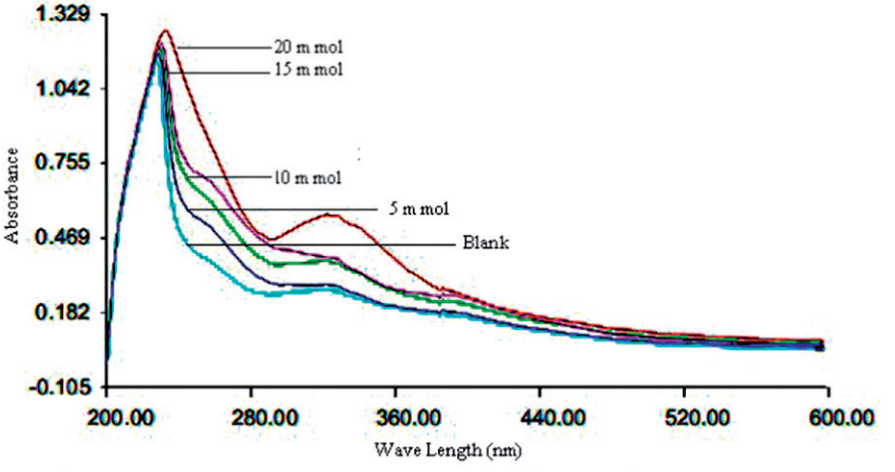

Blank = without DNA; 5, 10, 15 and 20 mmol = Concentration of CT-DNA in micromoles.

Figure 1. Absorption titration of $[RuCO(PPh_3)L^2]$ with CT-DNA.

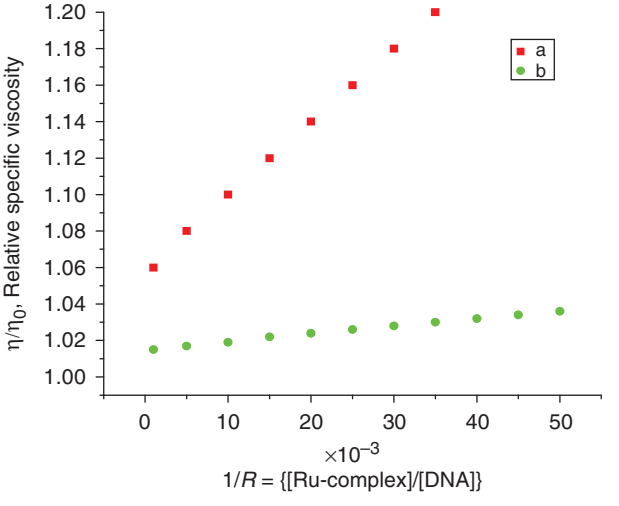

Figure 2. The effect of (a) $[RuCO(PPh_3)L^2]$ and (b) CT-DNA on the viscosity of CT-DNA at $1/R = 0.5$ relative viscosity *vs.* $1/R$.

4. Conclusion

A group of mononuclear octahedral ruthenium(II) Schiff-base complexes have been synthesized. All ruthenium(II) Schiff-base complexes have been examined for their catalytic efficiency in oxidation of alcohols to their corresponding carbonyl compounds with molecular oxygen at room temperature and also for C–C coupling reactions. Compared to previous literature [57,58], certain newly synthesized complexes show good antibacterial activity, higher than their respective standards. Finally, with

absorption titration studies and viscosity measurements, it can be concluded that the complexes bind to CT-DNA through intercalation.

References

[1] T.D. Thangadurai, S. Jeong, S. Yun, S. Kim, C. Kim, Y.I. Lee. *Micro. Chem. J.*, **95**, 235 (2010).
[2] M. Wang, L.F. Wang, Y.Z. Li, Q.X. Li, Z.D. Xu, D.M. Qu. *Transition Met. Chem.*, **26**, 307 (2001).
[3] A. Chipeleme, J. Gut, P.J. Rosenthal, K. Chibale. *Bioorg. Med. Chem.*, **15**, 273 (2007).
[4] R.K. Agarwal, S. Prasad. *Turk. J. Chem.*, **29**, 289 (2005).
[5] S.B. Padhye, G.B. Kauffman. *Coord. Chem. Rev.*, **63**, 127 (1985).
[6] D.X. West, A.E. Liberta, S.B. Padhye, R.C. Chikate, P.B. Sonawane, A.S. Kumbhar, R.G. Yerande. *Coord. Chem. Rev.*, **123**, 49 (1993).
[7] Y.P. Tian, C.Y. Duan, Z.L. Lu, X.Z. You, H.K. Fun, S. Kandhasamy. *Polyhedron*, **15**, 2263 (1996).
[8] T. Rosu, A. Gulea, A. Nicolae, R. Georgescu. *Molecules*, **12**, 782 (2007).
[9] P.Z. Saiz, J.G. Tojal, A. Mendia, B. Donnadieu, L. Lezama, J.L. Pizarro, M.I. Arriortna, T. Roza. *Eur. J. Inorg. Chem.*, 518 (2003).
[10] M. Mohan, A. Agarwal, N.K. Jha. *J. Inorg. Biochem.*, **34**, 41 (1988).
[11] H.N. Tang, L.F. Wang, R.D. Yang. *Transition Met. Chem.*, **28**, 395 (2003).
[12] D.R. Prasad, G. Ferraudi. *J. Phys. Chem.*, **86**, 4037 (1982).
[13] D.A. Cogan, G.C. Liu, K.J. Kim, B.J. Backes, J.A. Ellman. *J. Am. Chem. Soc.*, **120**, 8011 (1998).
[14] T. Punniyamurthy, S. Velusamy, I. Javed. *Chem. Rev.*, **105**, 2329 (2005).
[15] M. Pagliaro, S. Campestrinian, R. Ciriminna. *Chem. Soc. Rev.*, **34**, 837 (2005).
[16] K.E. Erkkila, D.T. Odom, J.K. Barton. *Chem. Rev.*, **99**, 2777 (1999).
[17] C. Metcalfe, J.A. Thomas. *Chem. Soc. Rev.*, **32**, 215 (2003).
[18] Y. Xiong, L.N. Ji. *Coord. Chem. Rev.*, **185**, 711 (1999).
[19] A.I. Vogel. *Text Book of Practical Organic Chemistry*, 5th Edn, p. 264, Longman, London (1989).
[20] N. Ahmed, J.J. Levision, S.D. Robinson, M.F. Uttely. *Inorg. Synth.*, **48**, 15 (1974).
[21] R.A. Sanchez-Delgado, W.Y. Lee, S.R. Choi, Y. Cho, M.J. Jun. *Transition Met. Chem.*, **16**, 241 (1991).
[22] S. Gopinathan, I.R. Unny, S.S. Deshpande, C. Gopinathan. *Ind. J. Chem.*, **25A**, 1015 (1986).
[23] G. Asgedom, A. Sreedhara, J. Kivikoshi, C.P. Rao. *Polyhedron*, **16**, 643 (1997).
[24] G. Nageswara Rao, C.H. Janardhana, K. Pasupathy, P. Mahesh Kumar. *Ind. J. Chem.*, **39B**, 5 (2000).
[25] A.N. Bauer, W.M.M. Kirby, J.C. Sherries, M. Truck. *Am. J. Clin. Pathol.*, **45**, 493 (1996).
[26] J. Marmur. *J. Mol. Biol.*, **3**, 208 (1961).
[27] M.F. Reichmann, S.A. Rice, C.A. Thomas, P. Doty. *J. Am. Chem. Soc.*, **76**, 3047 (1954).
[28] F.A. Beckford, G. Leblanc, J. Thessing, M. Shaloski Jr, B.J. Frost, L. Li, N.P. Seeram. *Inorg. Chem. Commun.*, **12**, 1094 (2009).
[29] K.P. Deepa, K.K. Aravindakshan. *Synth. React. Inorg. Met. Org. Chem.*, **30**, 1601 (2000).
[30] M. Gomez Andreu, A. Zapf, M. Beller. *Chem. Commun.*, 2475 (2000).
[31] S.A. Ali, A.A. Soliman, M.M. Aboaly, R.M. Ramadan. *J. Coord. Chem.*, **55**, 1161 (2002).
[32] R.C. Maurya, P. Patel, S. Rajput. *Synth. React. Inorg. Met. Org. Chem.*, **23**, 817 (2003).
[33] M.S. El-Shahawi, A.F. Shoair. *Spectrochim. Acta*, **60A**, 121 (2004).
[34] R. Ramesh, M. Sivagamasundari. *Synth. React. Inorg. Met. Org. Chem.*, **33**, 899 (2003).
[35] A.B.P. Lever. *Inorganic Electronic Spectroscopy*, 2nd Edn, Elsevier, New York (1984).
[36] K. Chichak, U. Jacquennard, N.R. Branda. *Eur. J. Inorg. Chem.*, 357 (2002).
[37] K. Natarajan, R.K. Poddar, C. Agarwala. *J. Inorg. Nucl. Chem.*, **39**, 431 (1977).
[38] J.S. Casas, M.V. Castaro, M.C. Cifuentes, J.C. Garcia-Monteagudo. *J. Org. Met. Chem.*, **692**, 2234 (2007).
[39] P. Barbazan, R. Carballo, I. Prieto, M. Turnes, E.M. Vazquez-Lopez. *J. Organomet. Chem.*, **694**, 3102 (2009).
[40] M. Sivagamasundari, R. Ramesh. *Spectrochim. Acta*, **66A**, 427 (2007).
[41] C. Jayabalakrishnan, R. Karvembu, K. Natarajan. *Synth. React. Inorg. Met. Org. Chem.*, **33**, 1535 (2003).
[42] K.N. Kumar, R. Ramesh. *Polyhedron*, **24**, 1885 (2005).
[43] V. Mahalingam, N. Chitrapriya, F.R. Fronczek, K. Natarajan. *Polyhedron*, **27**, 1917 (2008).
[44] D. Chatterjee, A. Mitra, B.C. Roy. *J. Mol. Catal. A Chem.*, **17**, 161 (2000).
[45] K. Srinivasan, P. Michand, J.K. Kochi. *J. Am. Chem. Soc.*, **108**, 2309 (1986).
[46] P.K. Bhattacharya. *Proc. Indian Acad. Sci. (Chem. Sci.)*, **102**, 247 (1990).
[47] R. Karvembu, S. Hemalatha, R. Prabhakaran, K. Natarajan. *Inorg. Chem. Commun.*, **6**, 486 (2003).
[48] D. Chatterjee, A. Mitra, S. Mukherjee. *J. Mol. Catal. A Chem.*, **165**, 295 (2005).

[49] N. Sathya, A. Manimaran, G. Raja, P. Muthusamy, K. Deivasigamani, C. Jayabalakrishnan. *Transition Met. Chem.*, **34**, 7 (2009).
[50] C. Perez, M. Pauli, P. Bezerque. *Acta Biol. Med. Exp.*, **15**, 113 (1990).
[51] A. Katritzky. *Comprehensive Heterocyclic Chemistry*, Vol. 4, Pergamon Press, New York (1984).
[52] R.S. Srivastava. *J. Inorg. Nucl. Chem.*, **42**, 1526 (1990).
[53] B.G. Tweedy. *Phytopathology*, **55**, 910 (1964).
[54] S.C. Sing Jadon, N. Gupta, R.V. Singh. *Ind. J. Chem.*, **34A**, 733 (1995).
[55] T.D. Thangadurai, K. Natarajan. *Ind. J. Chem.*, **41A**, 741 (2002).
[56] D. Herebian, W.S. Sheldrick. *J. Chem. Soc., Dalton Trans.*, 966 (2002).
[57] S. Ramakrishnan, M. Palaniandavar. *J. Chem. Sci.*, **117**, 179 (2005).
[58] M.S. Deshpande, A.A. Kumbhar, A.S. Kumbhar, M. Kumbhakar, H. Pal, U.B. Sonawane, R.R. Joshi. *Bioconjugate Chem.*, **20**, 447 (2009).